

## Inversion of sound speed profiles from MBES measurements using Differential Evolution

Keyzer, L.M.; Mohammadloo, Tannaz H.; Snellen, M.; Pietrzak, J.D.; Katsman, C.A.; Afrasteh, Y.; Guarneri, H.; Verlaan, M.; Klees, R.; Slobbe, D.C.

**DOI**

[10.1121/2.0001508](https://doi.org/10.1121/2.0001508)

**Publication date**

2021

**Document Version**

Final published version

**Published in**

Proceedings of Meetings on Acoustics 2021

**Citation (APA)**

Keyzer, L. M., Mohammadloo, T. H., Snellen, M., Pietrzak, J. D., Katsman, C. A., Afrasteh, Y., Guarneri, H., Verlaan, M., Klees, R., & Slobbe, D. C. (2021). Inversion of sound speed profiles from MBES measurements using Differential Evolution. In *Proceedings of Meetings on Acoustics 2021* (1 ed., Vol. 44) <https://doi.org/10.1121/2.0001508>

**Important note**

To cite this publication, please use the final published version (if applicable). Please check the document version above.

**Copyright**

Other than for strictly personal use, it is not permitted to download, forward or distribute the text or part of it, without the consent of the author(s) and/or copyright holder(s), unless the work is under an open content license such as Creative Commons.

**Takedown policy**

Please contact us and provide details if you believe this document breaches copyrights. We will remove access to the work immediately and investigate your claim.

***Green Open Access added to TU Delft Institutional Repository***

***'You share, we take care!' - Taverne project***

**<https://www.openaccess.nl/en/you-share-we-take-care>**

Otherwise as indicated in the copyright section: the publisher is the copyright holder of this work and the author uses the Dutch legislation to make this work public.

# Inversion of sound speed profiles from MBES measurements using Differential Evolution

Lennart Keyzer, Tannaz H. Mohammadloo, Mirjam Snellen, et al.

Citation: *Proc. Mtgs. Acoust.* **44**, 070035 (2021); doi: 10.1121/2.0001508

View online: <https://doi.org/10.1121/2.0001508>

View Table of Contents: <https://asa.scitation.org/toc/pma/44/1>

Published by the [Acoustical Society of America](#)

---

## ARTICLES YOU MAY BE INTERESTED IN

[Comparison of methods employed to extract information contained in seafloor backscatter](#)

*Proceedings of Meetings on Acoustics* **44**, 070036 (2021); <https://doi.org/10.1121/2.0001509>

[Multi-UUV object detection, localization and tracking with secure, full-duplex communication networks](#)

*Proceedings of Meetings on Acoustics* **44**, 070037 (2021); <https://doi.org/10.1121/2.0001510>

[A dataset of underwater passive acoustic recordings from a 2-year mooring deployment in Fram Strait \(UNDER-ICE\)](#)

*Proceedings of Meetings on Acoustics* **44**, 070034 (2021); <https://doi.org/10.1121/2.0001507>

[Throughput enhancement using Hierarchical Modulation for Underwater Acoustic Communication System](#)

*Proceedings of Meetings on Acoustics* **44**, 070027 (2021); <https://doi.org/10.1121/2.0001495>

[Remote acoustic detection and characterization of fish schooling behavior](#)

*The Journal of the Acoustical Society of America* **150**, 4329 (2021); <https://doi.org/10.1121/10.0007485>

[The calculation of acoustic field in a metamaterial and determination of its inner structure using scattering coefficients](#)

*Proceedings of Meetings on Acoustics* **42**, 065005 (2020); <https://doi.org/10.1121/2.0001514>

---



**Advance your science and career  
as a member of the**

**ACOUSTICAL SOCIETY OF AMERICA**

LEARN MORE





## 6th Underwater Acoustics Conference & Exhibition

20-25 June 2021

**Underwater Acoustics: Multibeam Echo  
Sounding: Bathymetry and sediment Classification**

# Inversion of sound speed profiles from MBES measurements using Differential Evolution

**Lennart Keyzer, Tannaz H. Mohammadloo, Mirjam Snellen, Julie Pietrzak, Caroline Katsman, Yosra Afrasteh, Henrique Guarneri, Martin Verlaan, Roland Klees, and Cornelis Slobbe**

*Delft University of Technology: Technische Universiteit Delft, Delft, Zuid-Holland, 2628 CN, NETHERLANDS; l.m.keyzer@tudelft.nl; T.HajiMohammadloo@tudelft.nl; m.snellen@tudelft.nl; j.d.pietrzak@tudelft.nl; C.A.Katsman@tudelft.nl; y.afrasteh@tudelft.nl; h.guarneri@tudelft.nl; m.verlaan@tudelft.nl; R.Klees@tudelft.nl; d.c.slobbe@tudelft.nl*

The sound speed provides insight in ocean properties, as it depends on depth, temperature and salinity. Here, we propose a method to invert sound speed profiles (SSPs) from multibeam echosounder (MBES) measurements, providing a SSP for every ping. Using erroneous SSPs results in a mismatch in the estimated bathymetry between overlapping swaths. The SSP is estimated by minimizing this mismatch using Differential Evolution. In this work, SSPs are described using empirical orthogonal functions (EOFs), which are obtained from historical SSPs. As a proof-of-concept, we apply the inversion on a simulated MBES survey, where the synthetically generated SSPs are fully described by 3 EOFs. The inverted SSPs deviate 1 m/s from the correct profiles. In the case of actual SSPs, more EOFs are possibly required. The number of required EOFs to get an accurate estimate of the SSP is assessed by using SSPs acquired in the North Sea. Results show that including only 2 EOFs is sufficient to accurately estimate the SSP, although larger deviations up to 3 m/s were found. In this paper, we demonstrated the potential of the proposed method to invert SSPs from MBES measurements, which can provide information about the vertical structure of the water column.

---

## 1. INTRODUCTION

Estuaries and river plumes are highly dynamic areas. Due to the input of fresh river water, strong salinity and/or temperature gradients arise both vertically and horizontally. The resulting density differences induce complex currents, which affect, among others, salt intrusion and sediment transport<sup>1</sup>.

Measuring these phenomena is a challenge. To capture the strong variability in both time and space, very extensive measurement campaigns are required. The deployment of moorings would cover the temporal variability at fixed locations, but not capture the spatial variability. In contrast, vessels are able to cover a larger spatial domain, but many surveys would be required to increase the temporal coverage.

To ensure nautical safety, bathymetric surveys are conducted regularly. This is often done using multibeam echosounders (MBES). A ping is transmitted in a wide swath perpendicular to the sailing direction. Beamforming at reception allows to estimate depths from the two-way travel time and beam angle, in combination with a sound speed profile (SSP). This SSP is measured independently by lowering a sound velocity profiler or a Conductivity-Temperature-Depth (CTD) measurement device. Since these measurements are time-consuming, typically only a few are taken per survey.

In case an erroneous SSP is used, the bathymetry estimated from the two-way travel times will be deformed. These deformations are typically known as smileys or frownies because of the convex shape of the estimated bathymetry along a swath. The deviation is largest for the outer beams. To minimize this error in the estimated bathymetry and to meet the IHO standards for hydrographic operations, it is common practice that the swaths overlap by sailing adjacent tracks sufficiently close to each other. Since the time between measuring two overlapping swaths is generally much smaller than the typical timescale of bed level changes, the bottom can be assumed stable. In case a mismatch is observed between the water depth estimates of the overlapping swaths, it can thus be associated to the use of erroneous SSPs. Mohammadloo *et al.*<sup>2</sup> utilized this redundancy to correct the bathymetric measurements by minimizing the mismatch in water depth estimates between overlapping swaths. They parametrized the SSP using a mean sound speed and a constant gradient.

In this study, we propose a method to invert the SSP from MBES measurements, following a similar approach as Mohammadloo *et al.* used to estimate the bathymetry<sup>2</sup>. In contrast, we parametrize the SSP using a series of basis functions, i.e. empirical orthogonal functions (EOFs), such that it can be described by a limited number of variables. The EOFs can be derived for specific areas if a sufficient number of historically collected SSPs is available. Typically, only a few EOFs are needed to accurately describe the profiles for that specific area and season, assuming that the historical data are still appropriate. Our method allows to estimate the SSP for each ping, providing large sets of SSPs. This gives insight in the temporal and spatial variability of the sound speed in the area of interest. Since the sound speed is governed by depth, temperature and salinity, changes in the sound speed reflect variations in the salinity and/or temperature. Exploiting MBES measurements by inverting the SSP can thus provide additional oceanographic data.

In Section 2 we give a detailed explanation of the proposed method. Subsequently, we invert the SSPs from a simulated MBES survey, where synthetic SSPs are used that are fully described by 3 EOFs. This proof-of-concept is presented in Section 3. In Section 4, we investigate the required number of EOFs to get an accurate estimate of the SSP. To this end, the synthetic SSPs in the simulated MBES survey are replaced by historically measured SSPs. The conclusions are presented in Section 5.

## 2. METHOD

In this section, we elaborate on the proposed method to invert SSPs from MBES measurements in more detail. The inversion is based on the fact that using an erroneous SSP results in a convex-shaped estimate of the bathymetry when processing MBES measurements. In Fig. 1, we illustrate how this results in a mismatch in the estimated bathymetry between two overlapping swaths by adopting erroneous SSPs and subsequently determining the bathymetry using a ray tracing algorithm. The bottom is assumed to be stable. We quantify this mismatch using a so-called energy function (Section 2A). The SSPs are estimated by minimizing this energy function using Differential Evolution (DE) (Section 2B). To limit the number of unknowns, the SSPs are described using EOFs (Section 2C). The inversion gives an SSP for each ping along each track, providing large datasets.

---

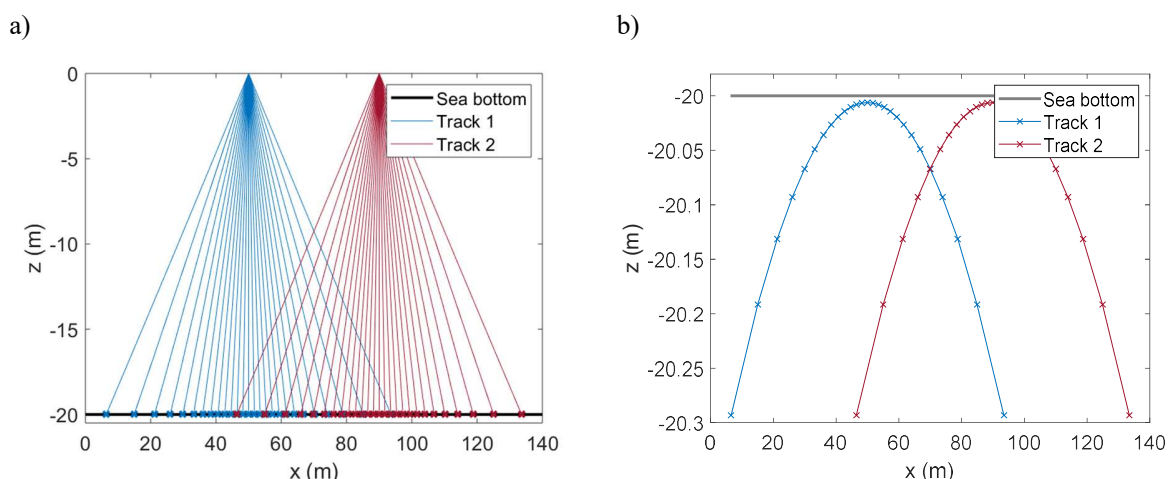


**Figure 1. a) Two overlapping MBES swaths; b) The deformation of the estimated bathymetry for the two swaths due to the use of erroneous SSPs, resulting in a mismatch in the estimated bathymetry between the overlapping swaths (between  $x = 45$  m and  $x = 95$  m).**

## A. ENERGY FUNCTION

The fitness of a SSP is evaluated using the energy function, which quantifies the mismatch in estimated bathymetry between overlapping swaths. The energy function ( $E$ ) is defined as

$$E = \sum_j \sqrt{\frac{\sum_k (\hat{z}_{j,k} - z_{j,k})^2}{K}}, \quad (1)$$

where  $z_{j,k}$  is the real depth,  $\hat{z}_{j,k}$  the estimated depth per beam  $k$  of track  $j$ , and  $K$  is the total number of beams.  $\hat{z}_{j,k}$  is obtained using a ray tracing algorithm and depends on the SSP. Of course, the real depth is not known in practice. Therefore,  $z_{j,k}$  is obtained by combining and interpolating the depth estimates of the different swaths. The more accurate the SSPs are, the smaller the mismatch between overlapping swaths will be, and the lower  $E$  will be.

This energy function is a modified version of the one used by Mohammadloo *et al.*<sup>2</sup>. Since the depth estimates are no longer gridded and averaged, it is expected to improve the estimate of the SSP, especially in case of irregular bathymetry. The energy function is computed per segment. A segment consists of one ping per track. It is required that all tracks are parallel and sufficiently close to each other, such that the swaths of the different pings in each segment are aligned and overlap. This definition is, therefore, less versatile applicable than the one that is used by Mohammadloo *et al.*<sup>2</sup>, since vessels are subject to pitch and yaw.

## B. DIFFERENTIAL EVOLUTION

The search for the best SSP is an optimization problem; the energy function is minimized. Here, we use the global optimization method Differential Evolution (DE). This algorithm was developed by Storn & Price<sup>3</sup>, and has been applied successfully to other inversion problems before<sup>2,4</sup>.

DE is a subset of the well-known genetic algorithms. It searches for the global optimum, i.e. the SSP for which the energy function is minimal, by improving the solution iteratively based on an evolutionary process. The first generation is defined randomly, respecting the search bounds for the unknown parameters. A generation, i.e. an iteration, consists of a number of candidate solutions, depending on the population size. A candidate solution consists of a SSP per track. For every candidate solution, the bathymetry is determined using a ray tracing algorithm and next the energy function is evaluated. Subsequent generations are defined based on a process of mutation, crossover, and selection. Different variants of DE exist, which apply different mutation schemes<sup>5</sup>. Here, we use the classical DE/rand/1/bin scheme. The population is mutated by adding the weighted difference between two randomly chosen members to a third one. The process of crossover determines which mutations are passed down to the next generation. For this scheme, the crossover probability is binomially distributed. A population member enters the next generation if it outperforms its predecessor. The algorithm is terminated when a preset maximum number of generations is exceeded. For further details on the application of the DE algorithm on inversion problems, we refer to the work of Snellen & Simons<sup>4</sup>.

The performance of DE, i.e. the probability to locate the global optimum, is highly determined by the so-called setting parameters:

- Mutation scheme
- Multiplication factor
- Crossover rate
- Population size
- Maximum number of generations

The DE setting parameters as used in this study can be found in Table 1. The values for the multiplication factor and crossover probability were set as used by Mohammadloo *et al.*<sup>2</sup> and Snellen & Simons<sup>4</sup>. The population size and maximum number of generations were set to 32 and 300 respectively, to avoid preliminary termination of the optimization.

**Table 1. DE settings**

Mutation scheme	DE/rand/1/bin
Multiplication factor	0.6
Crossover probability	0.55
Population size	32
Max. number of generations	300

### C. EOF ANALYSIS

The unknowns we need to find using DE are the SSPs for the different tracks. An SSP is, however, a continuous profile over depth, which implies that the number of unknowns is infinite. To limit the number of unknowns, we make use of EOFs, which are determined from measured SSPs. They constitute a set of orthogonal basis functions from which the measured SSPs can be reconstructed.

Each measured SSP ( $c_n$ ) can be described by

$$c_n = \bar{c} + \sum_m p_{m,n} v_m, \quad (2)$$

where  $\bar{c}$  is the mean SSP of the dataset,  $p_{m,n}$  the  $m^{\text{th}}$  EOF coefficient of the  $n^{\text{th}}$  SSP and  $v_m$  the  $m^{\text{th}}$  EOF. The EOFs are the eigenvectors of the covariance matrix  $R$ , which is defined as

$$R = \frac{1}{N} \sum_{n=1}^N [c_n - \bar{c}][c_n - \bar{c}]^T, \quad (3)$$

where  $N$  is the total number of SSPs. Subsequently, the EOF coefficients  $p$  follow from

$$p_{m,n} = V^{-1}[c_n - \bar{c}], \quad (4)$$

where  $V$  is the matrix containing the eigenvectors of the covariance matrix.

We can approximate an SSP using the  $G$  largest eigenvalues by

$$\tilde{c}_n = \bar{c} + \sum_{m=1}^G p_{m,n} v_m. \quad (5)$$

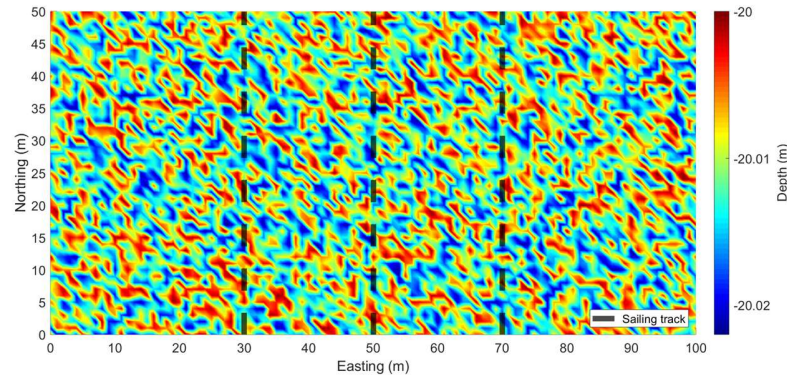
In this way, SSPs can be constructed using a limited number of variables, instead of needing to define the sound speed at every point in depth. This simplifies the candidate solutions in DE to a vector with EOF coefficients, which length depends on the number of EOFs and the number of tracks.

### 3. PROOF-OF-CONCEPT

As a proof-of-concept, we start with the inversion of a set of synthetically generated SSPs from a simulated MBES survey. We consider a rectangular domain with a constant depth of 20 m including white noise with an amplitude of 2.2 cm (Fig. 2a). The MBES survey is simulated by sailing three parallel tracks through the domain in north-south direction (dashed black lines). Along each track, a ping is emitted every 5 m and the swaths overlap for 70%. In order to calculate the travel times, a SSP is required. For this simulation, synthetic SSPs are generated using 3 EOFs, which are obtained after performing an EOF analysis on an existing dataset of 288 measured SSPs. The EOF coefficients are randomly generated within the range of the coefficients of the original SSPs. The resulting synthetic SSPs are shown in Fig. 2b. The sound speed varies over depth between 1455 m/s

and 1475 m/s. Subsequently, the travel time per beam for every ping is computed using a ray tracing algorithm. Since this survey consists of 3 tracks and 3 EOF coefficients per SSP are required, 9 unknowns need to be estimated per segment.

a)



b)

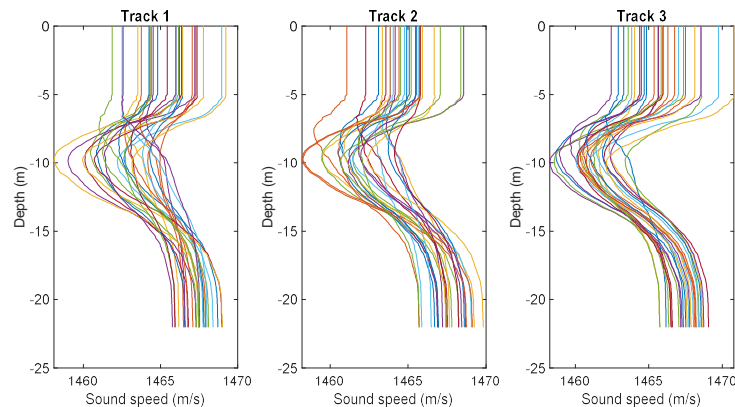


**Figure 2. a) The domain with a depth of 20 m and the three sailed tracks (black dashed lines). b) The synthetic SSPs per track that are used to calculate the travel times for each ping.**

Fig. 3a shows the inverted SSPs (dashed lines) of the first ping of each track, estimated using the algorithm described in Section 2 together with the correct SSPs (solid lines). The maximum deviation is less than 1 m/s. There is also good agreement between the vertical structure of the estimated SSP and the correct SSP. To inspect the performance of the inversion, we can also check the estimated bathymetry (Fig. 3b and c). The difference between the bathymetry estimated using the inverted SSPs and the correct bathymetry is in the order of millimetres. This is much smaller than the IHO standards for hydrographic surveys; the maximum total vertical uncertainty is 0.18 m for NL order A, assuming a depth of 20 m. Fig. 4 shows the inverted SSPs for the first 10 pings along the first track. Again, we find a good agreement in the vertical structure of the SSPs and a maximum deviation of 1 m/s. Similar results are found for track 2 and 3 (not presented here).

So for this idealized case, the results indicate that the proposed method is able to successfully invert the SSPs from MBES measurements. A major simplification, however, is that these synthetic SSPs can be fully described using only three EOFs. In reality, more EOFs might be required to accurately describe the SSPs. The more EOFs are needed, the more unknowns need to be found, which will complicate the inversion. An important question is, therefore, whether an accurate estimate of measured SSPs can be obtained if only a limited number of EOFs is included.



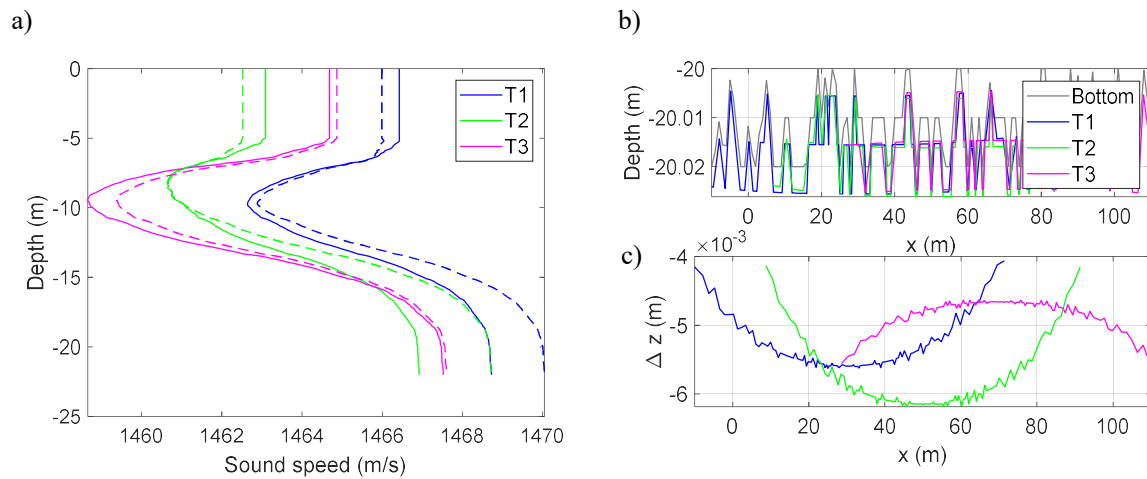


**Figure 3.** The results from the inversion for the first segment. *a)* The correct SSPs (solid lines) and the inverted SSPs (dashed lines) for the first ping of track 1 (blue), 2 (green), and 3 (magenta) ( $y = 0$  and  $x = 30, 50$  and  $70$  in Fig. 1a). *b)* The estimated bathymetry for each track. The grey line represents the bottom. *c)* The difference between the bottom and estimated bathymetry per track. Note the convex-shaped deformations as a result of the small deviations in the estimated SSP.

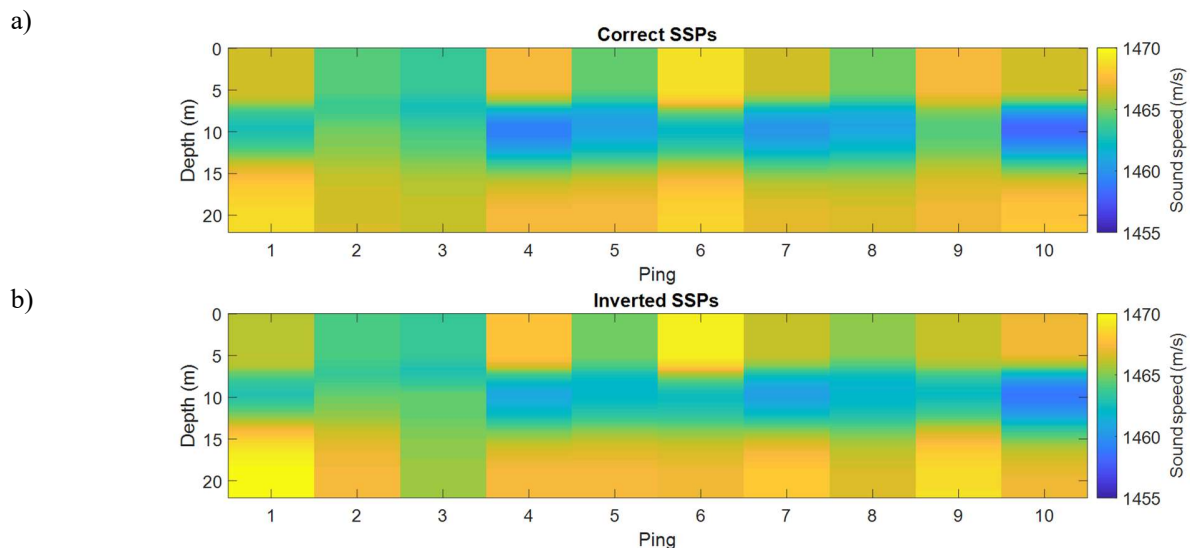


**Figure 4.** The correct SSPs (a) and the inverted SSPs (b) for all pings along track 1 ( $x = 30$  in Fig. 1a).

#### 4. NUMBER OF REQUIRED EOFs

In this section, we assess the number of required EOFs to get an accurate estimate of the SSP in case actual measured SSPs are used. To this end, we use the same MBES survey as in the previous section. However, we replace the synthetic SSPs by a dataset consisting of 65 measured SSPs, which is collected in the North Sea along the Dutch coast. For each ping, we randomly select a SSP from the dataset and recalculate the travel time. First, we explore the variability in the measured SSPs that is described by each EOF. Subsequently, we run the actual inversion including a varying number of EOFs.

The dataset of 65 historically collected SSPs is shown in Fig. 5a. First, we perform an EOF analysis on this dataset. Fig. 5b indicates the cumulative sum of eigenvalues, indicating what percentage of variation in the SSPs is accounted for by taking into account an increasing number of EOFs. In contrast to the synthetic SSPs, the first 3 EOFs explain now 96.3% of the variability in the measured SSPs. However, the fact that most of the variability

is already described by the first few EOFs suggests that including only a limited number of EOFs could result in an accurate estimate of the SSP. This would simplify the inversion.

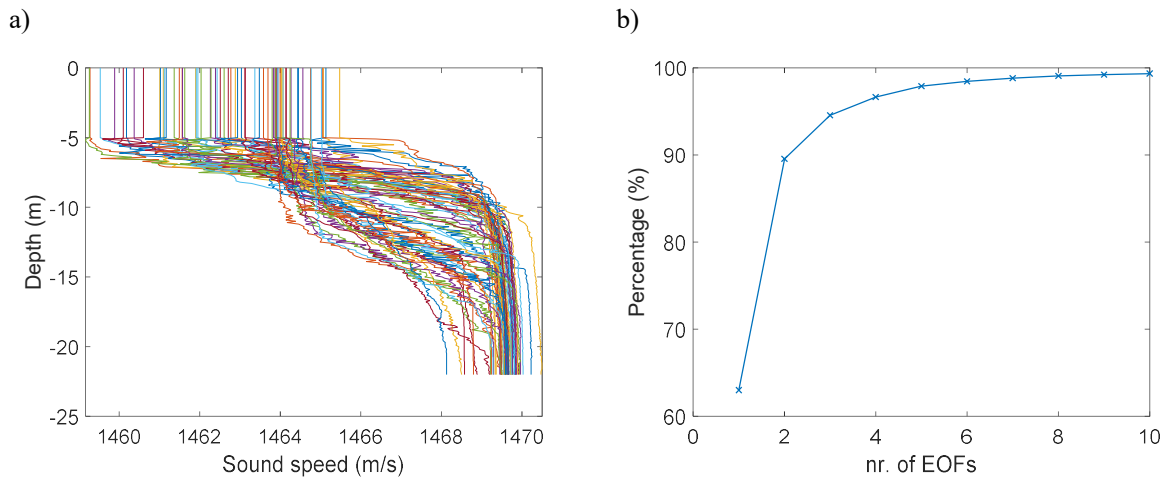


**Figure 5. a) Dataset of historically collected SSPs along Dutch coast. b) Cumulative percentage of the variability in sound speed explained by the number of included EOFs for this dataset.**

Next, we reconstruct the SSPs of the first ping of each track using an increasing number of EOFs. Subsequently, the bathymetry is determined and the energy function evaluated as a function of the number of EOFs (Fig. 6a – blue line). As expected, the energy reduces if more EOFs are included. However, it is found that more than 50 EOFs are required to approach the global minimum, i.e. the value of the energy function obtained using the measured SSPs (Fig. 6a – blue versus dashed black line). This is an unexpected result, however, as almost all of the variability was already described by the first 10 EOFs (Fig. 5b). If we take a closer look at the higher order EOFs, for example  $v_{20}$  (Fig. 6b), we find that these EOFs can be characterized as a noisy signal. These wiggles cannot be related to variations in temperature or salinity in the water column, while it can cause significant deformation of the estimated bathymetry. Therefore, we applied a 1-m moving average to remove the noise from the profiles. After computing the energy function again using the smoothed SSPs, it turns out that now only 12 EOFs are needed to approach the global minimum (Fig. 6a – orange versus dashed black line). Moreover, including only 2 EOFs results in a close approximation of the optimum already. This suggests again that only a limited number of coefficients needs to be found to obtain an accurate estimate of the SSPs.

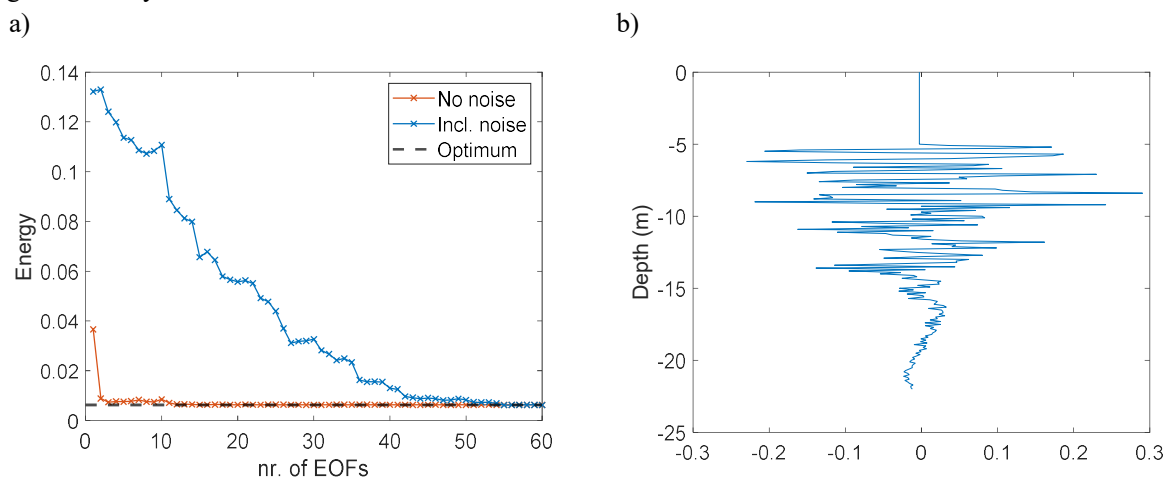


**Figure 6. a) The energy as a function of the number of included EOFs for two different cases: the measured SSPs including noise (blue line) and the smoothed SSPs (orange line). The SSPs are constructed using the correct EOF coefficients. The dashed line depicts the optimum, computed using the correct SSP. b) Example of a higher order EOF dominated by a noisy signal:  $v_{20}$ .**

To verify these findings, we carried out the actual inversion for the first segment several times, while including a varying number of EOFs. The same settings as in the previous simulation are used for DE (see Table 1). The results are presented in Fig. 7. Including more than 2 EOFs does not significantly improve the estimate of the SSP. The maximum deviation of 2 m/s is the same for 2, 3 and 4 EOFs and no significant improvement in the representation of the vertical structure is found. Also the value for the energy function does not decrease further. This shows that including only 2 EOFs in the inversion results in an accurate estimate of the SSP, confirming what was found in Fig. 6a.

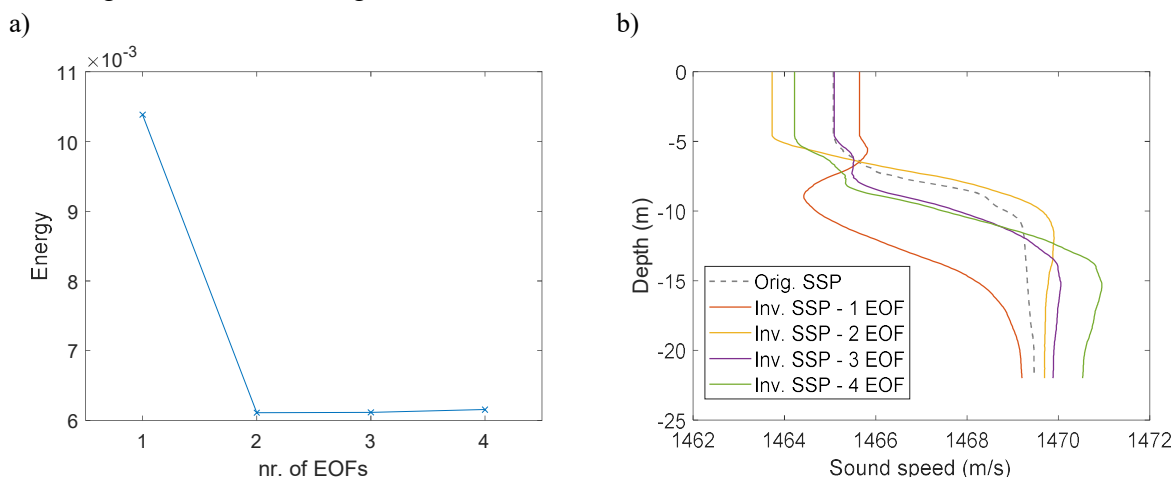


**Figure 7. Results from the inversion while including a varying number of EOFs, showing a) the energy and b) the inverted SSP for the first ping of the first track. The dashed line in (b) shows the correct SSP.**

To check the performance in more detail, the inversion including 2 EOFs is carried out for all pings. In Fig. 8, the results are shown for the first ping of all tracks. As a reference, we also plotted the SSPs approximated using Eq. (5) including 2 EOFs and the correct coefficients. The difference between these approximated profiles (solid lines) and the correct SSPs (grey dashed lines) is less than 0.4 m/s, confirming again that the profiles can be closely approximated by only 2 EOFs. Also the inverted SSPs (colored dashed lines) show strong agreement with the correct SSPs. Fig. 9 shows the estimated SSPs for the first 10 pings along the first track. The deviation from the correct sound speed near the bed is less than 0.5 m/s, while the surface sound speed deviates up to 3 m/s. In practice, however, the sound speed near the transducer at the surface is measured constantly which could be used to correct the inversion. In terms of ocean properties, this deviation of 3 m/s corresponds to a difference in salinity of about 2.5 PSU or in temperature of about 0.8 °C, based on Medwin's empirical relation for the sound speed in water<sup>6</sup>. Looking at the vertical structure, all SSPs show a strong vertical gradient between 5 m and 12 m. Although this gradient is reproduced in all estimated profiles, the depth at which this gradient is found differs up to 5 m. What causes this deviation requires further investigation, particularly since this depth will likely coincide with the pycnocline, which is an important ocean property. The bathymetry estimated using the inverted SSPs differs less than 5 cm from the correct bathymetry (not shown here), which is again far below the IHO requirements for vertical depth uncertainty of 18 cm. This indicates that the energy function is correctly minimized.

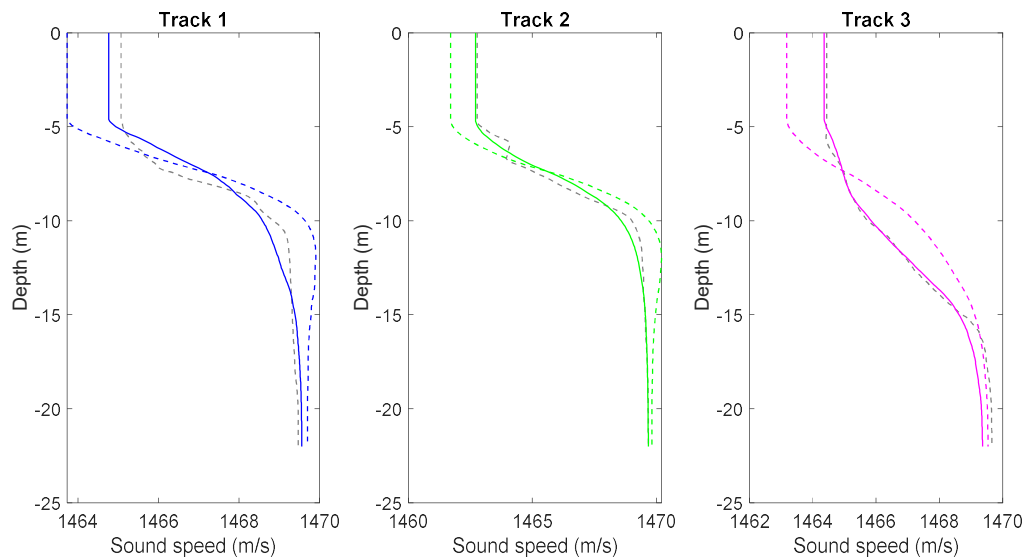


**Figure 8.** The inverted SSPs (dashed colored lines) for the first ping of track 1 (blue), 2 (green), and 3 (magenta) ( $y = 0$  and  $x = 30, 50$  and  $70$  in Fig. 1a). The solid colored lines depict the approximated SSP by Eq. (5) using 2 EOFs and the correct coefficients. The dashed grey lines are the correct SSPs.

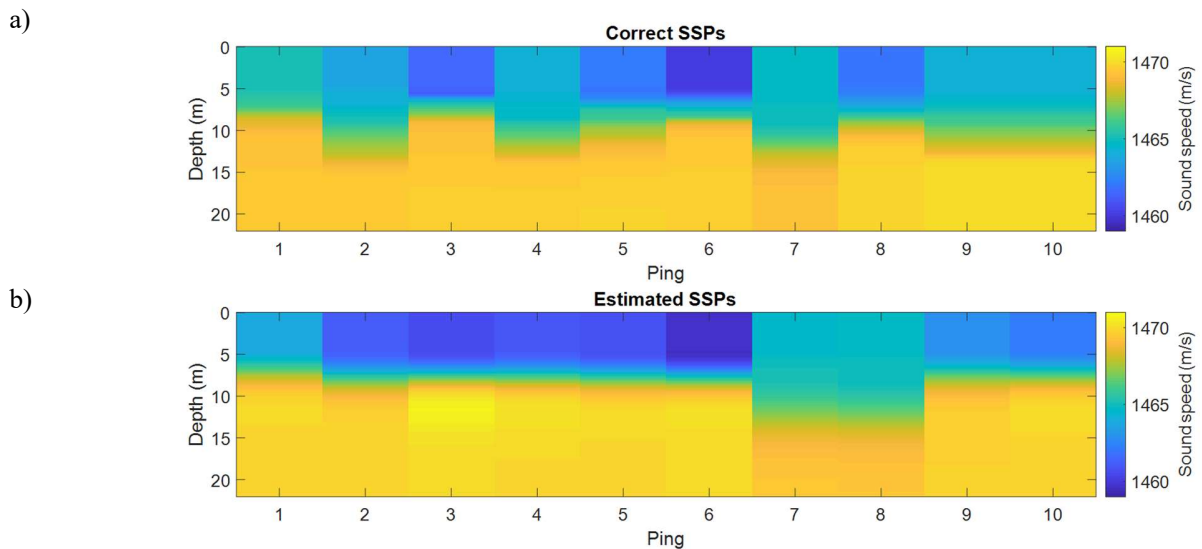


**Figure 9.** The correct SSPs (a) and the inverted SSPs (b) for all pings along the first track ( $x = 30$  in Fig. 1a).

## 5. CONCLUSION

Sound speed profiles provide valuable information on the vertical structure of the water column. Therefore, we propose a method to invert the sound speed profiles from MBES measurements. Using an energy function, we quantify the mismatch between overlapping swaths caused by the use of erroneous SSPs. The SSP is estimated by minimizing this energy function using Differential Evolution, a global optimization method. The use of empirical orthogonal functions allows us to describe the SSPs in an efficient way, as we can limit the number of unknowns that needs to be found during the inversion. This method provides a SSP for each ping of every track, resulting in datasets with high resolution in time and space.

In this study, we applied the inversion on two simulations of an MBES survey: one using synthetic SSPs that are fully described by 3 EOFs and one using historically collected SSPs near the Rhine-Meuse Delta. Both simulations showed promising results. The maximum deviation of the estimated SSPs was in the order of 1-3 m/s. In general, also good agreement in vertical structure was found, although the depth of the pycnocline, which

---

corresponds to a strong gradient in sound speed, was not always accurately reproduced for the second simulation. This requires further investigation. Furthermore, it was found that only 2 EOFs were required to get an accurate estimate of the SSP. The number of unknowns can thus be successfully limited by parameterizing the SSP using EOFs.

#### REFERENCES

- <sup>1</sup> M. A. de Nijs, J. D. Pietrzak, and J. C. Winterwerp, "Advection of the Salt Wedge and Evolution of the Internal Flow Structure in the Rotterdam Waterway," *Journal of Physical Oceanography*, **41**(1), 3-27 (2011), <https://doi.org/10.1175/2010JPO4228.1>.
- <sup>2</sup> T. H. Mohammadloo, M. Snellen, W. Renoud, J. Beaudoin and D. G. Simons, "Correcting Multibeam Echosounder Bathymetric Measurements for Errors Induced by Inaccurate Water Column Sound Speeds," *IEEE Access*, **7**, 122052-122068 (2019), <https://doi.org/10.1109/ACCESS.2019.2936170>.
- <sup>3</sup> M. Snellen, and D. G. Simons, "An assessment of the performance of global optimization methods for geo-acoustic inversion." *Journal of Computational Acoustics*, **16**(2), 199-223 (2008), <https://doi.org/10.1142/S0218396X08003579>
- <sup>4</sup> R. Storn, and K. Price, "Differential Evolution – A Simple and Efficient Heuristic for global Optimization over Continuous Spaces," *Journal of Global Optimization*, **11**, 341–359 (1997), <https://doi.org/10.1023/A:1008202821328>.
- <sup>5</sup> S. Das, and P. N. Suganthan, "Differential evolution: A survey of the state-of-the-art", *IEEE transactions on evolutionary computation*, **15**(1), 4-31 (2010), <https://doi.org/10.1109/TEVC.2010.2059031>.
- <sup>6</sup> H. Medwin, "Speed of sound in water: A simple equation for realistic parameters", *The Journal of the Acoustical Society of America*, **58**, 1318-1319 (1975), <https://doi.org/10.1121/1.380790>.